Article:

Weber, J. orcid.org/0000-0003-0643-2026, King, J.A. orcid.org/0000-0001-8825-0183, Abraham, N.L. orcid.org/0000-0003-3750-3544 et al. (7 more authors) (2024) Chemistry-albedo feedbacks offset up to a third of forestation's CO2 removal benefits. Science, 383 (6685). pp. 860-864. ISSN 0036-8075

https://doi.org/10.1126/science.adg6196

Chemistry-albedo feedbacks offset up to a third of forestation's CO_2 removal benefits.

James Weber[1]*, James A. King[1], Nathan Luke Abraham[2,3], Daniel P. Grosvenor[4,5], Christopher J. Smith[6,7], Youngsub Matthew Shin[2], Peter Lawrence[8], Stephanie Roe[9], David J. Beerling[1], Maria Val Martin[1]*

Affiliations:

[1]Leverhulme Centre for Climate Change Mitigation, School of Biosciences, University of Sheffield, Sheffield, S10 2TN, UK

[2]Centre for Atmospheric Science, Yusuf Hamied Department of Chemistry, University of Cambridge; Cambridge, CB2 1EW, United Kingdom.

[3]National Centre for Atmospheric Science, Yusuf Hamied Department of Chemistry, University of Cambridge; Cambridge, CB2 1EW, United Kingdom.

[4]Centre for Environmental Modelling and Computation (CEMAC), School of Earth and Environment, University of Leeds, Leeds, LS2 9JT, UK

[5]Met Office Hadley Centre, Exeter, UK

[6]Institute for Climate and Atmospheric Science, School of Earth and Environment, University of Leeds, Leeds, LS2 9JT, UK

[7]International Institute for Applied Systems Analysis, Laxenburg, Austria

[8]NCAR Earth System Laboratory, Climate and Global Dynamics Division, National Center for Atmospheric Research; Boulder, CO, USA

[9]World Wildlife Fund, Washington, DC, USA

*Corresponding authors. Emails: James Weber (j.weber@sheffield.ac.uk) and Maria Val Martin (m.valmartin@sheffield.ac.uk)

Abstract: Forestation is widely proposed for CO_2 removal but its impact on climate, via changes to atmospheric composition and surface albedo, remain relatively unexplored. We assess these responses using two Earth-System models by comparing a scenario with extensive global forest expansion in suitable regions to other plausible futures. We find forestation increases aerosol scattering and the greenhouse gases methane and ozone, following increased biogenic organic emissions, and decreases surface albedo which yields a positive radiative forcing (i.e. warming). This offsets up to a third of the negative forcing from the additional CO_2 removal under a 4°C warming scenario. However, when forestation is pursued alongside other strategies which achieve the 2°C Paris Agreement target, the offsetting positive forcing is smaller, highlighting the urgency for simultaneous emission reductions.

One-Sentence Summary: Extensive forestation changes atmospheric composition and surface reflectivity to offset a third of the extra CO_2 removal.

Forestation changes atmospheric composition and albedo to offset up to 1/3 of the extra CDR, depending on climate scenario.

Reforestation and afforestation are widely proposed nature-based strategies for atmospheric carbon dioxide (CO_2) removal (CDR) and climate change mitigation (*1*). These strategies have the potential to provide additional benefits for biodiversity and multiple ecosystem services, including reduced soil erosion and climate resilience, and forestry products and local cooling via transpiration (*2-4*). The Bonn Challenge, New York Declaration on Forests and the UN Decade on Ecosystem Restoration set a target to restore 350 Mha of degraded and deforested lands by 2030 (*5*). However, wide-scale forest expansion drives biophysical feedbacks within the Earth system that may lead to warming. For example, darker forests decrease surface albedo which can substantially offset the cooling effects of carbon sequestration in some regions of the world (*6,7*).

Forests also release substantial quantities (760 TgC yr^{-1}) of biogenic volatile organic compounds (BVOCs) that affect the greenhouse gases ozone (O_3) and methane (CH_4) as well as organic aerosols, with complex impacts on climate (*8,9*). Chemical reactions of BVOCs deplete the hydroxyl radical (OH), increasing CH_4, drive O_3 production or loss depending on the chemical environment, and produce oxidation products, which can add to or form aerosols that interact with solar radiation. Changes to atmospheric composition have been shown to be important in the net climatic impact of instantaneous global deforestation (*10*) and 1850-2000 deforestation due to cropland expansion (*11*). However, atmospheric composition's response to proposed reforestation and afforestation programmes under different 21st century future climate pathways, and the effects on climate, has received less consideration.

We present an assessment of climate feedbacks from a large-scale afforestation, reforestation and forest enhancement (hereafter all three are referred to as forestation) scenario. To mitigate possible single model bias (*8*), we perform the same experiments in two state-of-the-art climate models, UKESM1 (*12*) and CESM2 (*13*), which feature interactive atmospheric chemistry, aerosols and BVOC emission schemes. We use a land surface cover scenario that expands forests from 2015 land cover in biomes where trees are expected to thrive: through reforestation (of rangeland, secondary forest and secondary non-forest in forest biomes), forest enhancement (of forests where tree cover density is less than its potential), and afforestation (of rangeland, secondary forest and secondary non-forest in non-forest biomes where tree cover is greater than 10%) ("Maxforest" (MF)) (*14*). The Maxforest scenario represents a near biophysical maximum for forestation, given constraints on the rate of forestation and excluding expansion on croplands, pasturelands, urban lands and IUCN designated protected areas (SM Maxforest Scenario,). This scenario results in additional tree cover of 500 Mha by 2050 rising to 750 Mha in 2095 (relative to 2015) (Fig 1A), with approximately 55% from afforestation, 25% from reforestation, and 20% from forest enhancement by 2095. Although large-scale forestation presents certain risks and trade-offs (*1*), we use this theoretical biophysical maximum forestation scenario for our assessment to best detect biophysical changes.

We compare Maxforest to two well-established future scenarios: SSP3-7.0 ('Regional rivalry') which features resource-intensive consumption, diminished technology development and very low climate change mitigation efforts leading to global warming up to 4ºC above pre-industrial temperatures, and SSP1-2.6 ('Sustainability') characterised by inclusive development, environmental management, and lower resource and energy intensive consumption with much stronger efforts to mitigate climate change limiting warming to under 2°C (*15*). The land surface cover projection of SSP3-7.0 includes high levels of deforestation relative to 2015 (-290 Mha by 2095) while SSP1-2.6 has forestation which, at 310 Mha by 2095, is already 40% of the increase in Maxforest (Fig 1). The extensive mitigation efforts in SSP1-2.6 also lead to lower well-mixed greenhouse gas concentrations (CO_2, CH_4 and N_2O) than SSP3-7.0 and greater reductions to anthropogenic emissions of other climatically-relevant air pollutants such as NO_x (Fig S2,3; Table S1).

Specifically, we compare contemporaneous pairs of model simulations at 2050 and 2095 - a control run with land cover and atmospheric conditions from SSP3-7.0 or SSP1-2.6 (referred to as 4C_SSP3 and 2C_SSP1, respectively) and a run identical except for the substitution of land cover from Maxforest (4C_MF and 2C_MF, Table 1). These simulations use prescribed sea-surface temperatures and sea-ice.The land surface cover, described in terms of the fraction of each land surface type (trees, grassland, crops, urban etc) in each model grid cell, was fixed to scenario-specific values (Table 1). Thus, no deviation from the scenarios occurs over the course of the model simulations . This approach allows the effective radiative forcing to be calculated (16). However, the emissions of BVOCs from vegetation into the atmosphere are still interactively simulated based on the vegetation type, using the standard MEGAN (CESM2) (*17*) and iBVOC (UKESM1) (*18*) schemes, linking forestation to atmospheric composition. Thus, we isolate the effects of forestation on surface albedo and atmospheric chemical composition under two possible futures. We calculate the resulting change in the atmosphere's energy balance (the radiative forcing; RF) in 4C_MF and 2C_MF relative to the corresponding control simulation (4C_SSP3 & 2C_SSP1) with a focus on changes to surface albedo (RF_{Alb}), aerosol scattering (RF_{Aer}), CH_4 (RF_{CH4}) and O_3 (RF_{O3}). We compare this to the climatic impact of the extra CDR from Maxforest's additional forestation to establish the net climate benefit, calculated with CLM5, the CESM2 land surface component (Table S2), as Maxforest was originally developed within CESM2.

To isolate the effect of BVOC changes while ensuring comparability with the SSP pathways, we kept the fire and ozone induced-damage modules inactive in both UKESM1 and CESM2; i.e., we do not consider how fire emissions would respond to forestation nor the effect of surface ozone damage on forest carbon uptake (*19, 20)*. For fire emissions, we used the same prescribed biomass burning emissions for simulation pairs. For example, both 4C_SSP3 and 4C_MF scenarios use biomass burning emissions from SSP3-7.0 in 2050 and 2095 (see SM Earth Systems Model Simulations).

By embedding Maxforest's land surface cover into simulations using SSP3-7.0 and SSP1-2.6 atmospheric conditions, we provide thorough insights into forestation's impacts on atmospheric composition and climate in two contrasting futures. Our comprehensive analysis extends earlier work which considered the climatic impact of extensive forestation from CDR (e.g., (2*1*)) or, in some cases, albedo changes as well (*7*).

Results

We find the global net RF ($RF_{net} = RF_{Alb} + RF_{Aer} + RF_{CH4} + RF_{O3}$) from changes to surface albedo, aerosol scattering, CH_4 and O_3 from forestation is, in all cases, positive (i.e. corresponding to a warming) and relatively consistent between the models. Compared to 4C_SSP3, RF_{net} in 4C_MF is 90-104 mWm^{-2} (range here and throughout indicates the two-model range unless otherwise stated) by 2050, rising to 101-192mWm^{-2} by 2095 (Fig 3D). This is equivalent to CO_2 increases of 9-11 ppm (2050) and 16-30 ppm (2095) (Radiative Forcing Calculations, SM). The smaller increase in tree cover and BVOC emissions in 2C_MF relative to 2C_SSP1 leads to a smaller RF_{net} of 8-56mWm^{-2} at 2050 and 41-63 mWm^{-2} at 2095, equivalent to CO_2 increases of 1-5 ppm (2050) and 5-10 ppm (2095).

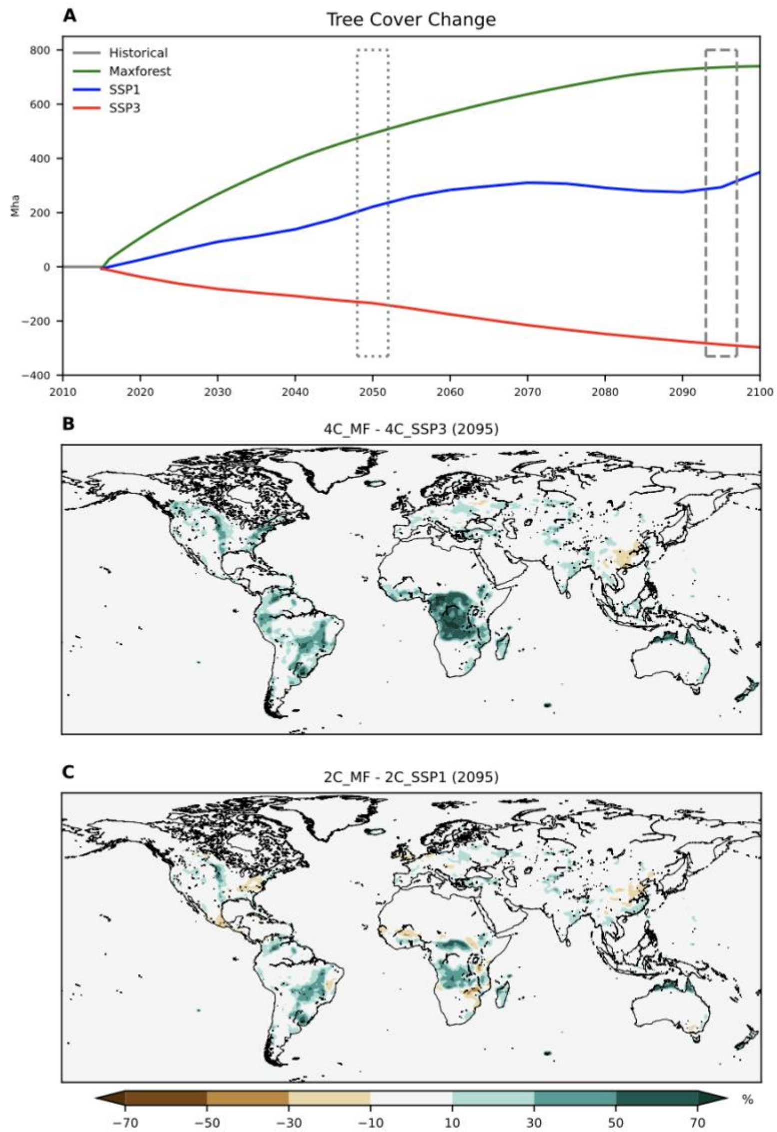

Fig. 1. Tree cover change. (A) Total tree cover change relative to the historical 2010-2014 mean for the Maxforest (MF), SSP3 and SSP1 land surface cover scenarios. Dotted and dashed boxes indicate time periods considered in this study (2050 and 2095). Also shown is the percentage difference in tree cover at 2095 between (**B**) 4C_MF and 4C_SSP3 and (**C**) 2C_MF and 2C_SSP1, corresponding to dashed region in (**A**).

Surface Albedo and Aerosol Scattering

We first assess the extent to which reductions in surface albedo arising from the expansion of forests (*22*), are offset by enhanced aerosol scattering following increases to organic aerosol produced from BVOC oxidation.

In the tropics, forest expansion leads to both models simulating positive RF_{Alb}, although the magnitude in UKESM1 is about twice that of CESM2 (Fig 2A,B, S6). The increase in BVOC emissions and thus organic aerosol from BVOC oxidation products (Fig S4,5) yields a negative forcing from aerosol scattering (RF_{Aer}) (Figs 2C, S6) which offsets some of the positive RF_{Alb}. The spatial distribution of RF_{Aer} correlates well with those regions exhibiting the greatest increases in organic aerosol. In 2095, under 4C and 2C conditions, aerosol scattering offsets about 50% of RF_{Alb} in UKESM1 and the entirety in CESM2 (Fig 3C,D).

At higher latitudes, the effect of forestation on surface albedo is more pronounced than in the tropics due to the lower albedo of forest and seasonal snow cover (which greatly increases albedo for periods of the year when snow can settle on non-forested land). As a result, the reduction in albedo per unit area of forestation is much higher than in the tropics. Furthermore, lower temperatures at higher latitudes limit the BVOC emissions (Fig 3B), resulting in reduced organic aerosol production and a smaller RF_{Aer}, meaning at higher latitudes the warming from surface albedo changes tends to outweigh the cooling from aerosol scattering (Fig 3C).

The greater RF_{Alb} per unit area of forestation at high latitude supports previous findings that high latitude forestation is likely to produce net warming due to albedo decreases (*22*). However, we extend this by illustrating how the cooling effect of aerosol scattering, particularly at lower latitudes, makes tropical forestation even more favourable, from a climatic perspective, by lowering its albedo penalty. Relative to 4C_SSP3 by 2095, RF_{Aer} in 4C_MF is -71 to -86 mWm^{-2} and RF_{Alb} 115-170 mWm^{-2} (Fig 3D). The smaller increase in forest cover in 2C_MF vs. 2C_SSP1 compared to 4C_MF vs. 4C_SSP3 (Fig 1) leads to smaller RF_{Aer} (-42 to -44 mWm^{-2}) and RF_{Alb} (57-84 mWm^{-2}) by 2095 (Fig S6). We note that UKESM consistently exhibits higher RF_{Alb}, highlighting the importance of a multi-model approach.

Changes to organic aerosol can also affect cloud properties, including reflectivity, albeit with the response highly sensitive to background cloud properties (*23*). Aside from a small region of central Africa, where the radiative impact is much smaller than the forcings from aerosol scattering and surface albedo changes, we find this effect statistically insignificant across almost the entire globe (SM Offline Cloud Forcing Calculations; Fig S7). While aerosol-driven changes to clouds appear relatively minor, the consideration of aerosol scattering and its partial offsetting of surface albedo-driven warming highlights the greater climatic benefits of tropical forestation and the need to assess the full range of processes by which forestation will affect the Earth System.

Methane and Ozone

The radiative impact of CH_4 changes (RF_{CH4}) from forestation is generally smaller in magnitude to that from aerosol scattering and opposite in sign (Fig 3D). OH is suppressed by reaction with elevated BVOC concentrations in both models, particularly in regions of forest expansion (Fig S8), reducing OH's destruction of CH_4 (Fig S9) and increasing CH_4 in both models. We find that forestation at 2095 results in a global positive RF_{CH4} of 32-57 mWm^{-2} for 4C_MF relative to 4C_SSP3 and 12-24 mWm^{-2} for 2C_MF relative to 2C_SSP1, with CESM2 exhibiting higher RF_{CH4} than UKESM1. Critically, the simulation of chemistry in both models features up-to-date descriptions of the chemistry of isoprene (the most widely emitted BVOC), including important reactions which regenerate OH and thus somewhat buffer its initial depletion (SM Earth System Model Simulations, SM).

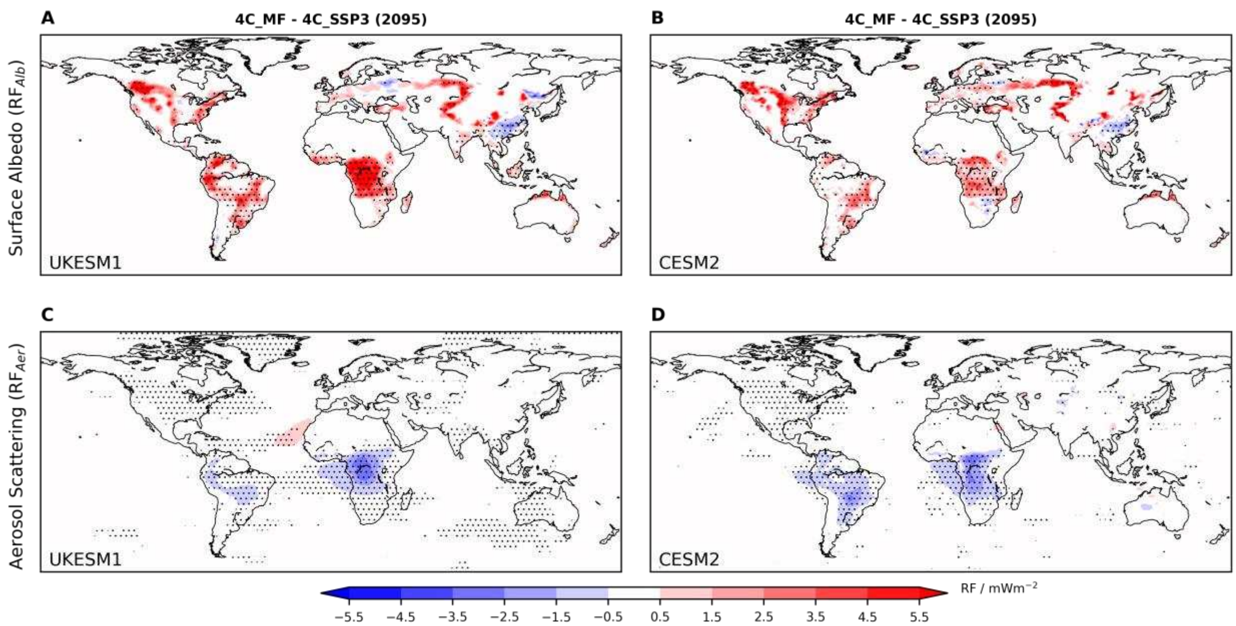

Fig. 2. Surface albedo and aerosol scattering. Radiative forcing from changes to surface albedo (RF_{Alb}) and the aerosol scattering (RF_{Aer}) between 4C_MF and 4C_SSP3 in (**A, C**) UKESM1 and (**B, D**) CESM2 at 2095. (Stippling shows regions of statistical significance at 95% confidence.)

The response of O_3 to BVOC changes is more complex than CH_4. RF_{O3} is positive in all cases, except SSP1-2.6 conditions in 2050 for CESM2 (i.e. 2C_MF vs. 2C_SSP1), with values of 7-20 wMWm^{-2} (rising to 60 wMWm^{-2} for 4C_MF vs. 4C_SSP3 in UKESM1 at 2095) albeit with greater interannual variation than RF_{CH4} due to the wide range of factors affecting O_3. A positive RF_{O3} with increasing BVOCs is in qualitative agreement with prior studies (*8,11*). The complexity of the O_3 response can be understood in terms of the strong dependence of net O_3 production on the local chemical environment and the fact that O_3 is much more efficient as a GHG in the upper troposphere than at lower altitudes (24). O_3 can be destroyed by direct reaction with BVOCs, produced in the presence of sufficient NO_x and destroyed again under very high NO_x via titration. This makes the net response highly dependent on regionally variable local conditions, on the pollution scenario (i.e., SSP3-7.0 has higher NO_x emissions than SSP1-2.6; Fig S3, Table S1) and, to a lesser extent, on the models due to differences in their chemical mechanisms. The climatic effect of ozone is generally comparable to that of CH_4 but smaller than the impact of aerosol scattering and surface albedo.

Carbon Dioxide Removal

Balancing the positive net radiative forcing from albedo and atmospheric composition changes is the additional CDR arising from the forest expansion in Maxforest (Figs S10-12). This forestation leads to an average CDR rate of 4.1-4.3 $GtCO_2$ yr^{-1} up to 2050 and 5.0-6.5 $GtCO_2$ yr^{-1} up to 2095 (with ranges for 2C and 4C conditions). This is within range of other estimates of biophysical and/or technical CDR potential of afforestation and reforestation of 0.5-10.1 $GtCO_2$ yr^{-1} by 2050 (*1*).

By 2095 Maxforest's CDR density (146 $tCha^{-1}$ and 184 $tCha^{-1}$ under 2C and 4C conditions, respectively) is also within the range of estimates from other 80-year widescale forestation studies, from 72 tC ha^{-1} from forestation of dryland regions (*7*) to ~200 and ~300 tC ha^{-1} reported by Bastin et al (2019) (*21*) (deserts, xeric shrublands and Mediterranean forests) and Griscom et al (2017) (*25*) respectively. The CDR density achieved by forestation is much smaller than that achieved by avoiding deforestation, which is about 500 tC ha^{-1} by 2095 in SSP3-7.0 (Methods). Thus preventing deforestation is much more efficient than reforestation in terms of mitigation per unit area.

To assess the importance of changes to surface albedo, aerosol scattering, CH_4 and O_3, we compare the sum of these components (RF_{net}) to the radiative forcing arising from the differences in cumulative CDR (and thus atmospheric CO_2) between the Maxforest scenarios and SSP3-7.0 or SSP1-2.6 (RF_{CO2}) (SM CDR Estimation). Under SSP3-7.0 conditions (4ºC warming), the enhanced biosphere carbon sink in Maxforest reduces atmospheric CO_2 by 84 ppm (656 $GtCO_2$) relative to SSP3-7.0 by 2095 (32 ppm., 234 $GtCO_2$ at 2050), causing a negative RF_{CO2} (i.e. a cooling) of -660 mWm^{-2} (-334 mWm^{-2} at 2050) (Fig 3E). However, the climatic impact of the non-CO_2 changes (RF_{net}) associated with the forestation negates 31±6% (at 2050) and 23±3% (at 2095) of this reduction (two-model mean with mean uncertainty), indicating that by 2095, Maxforest's forestation has only offset about 14% of SSP3-7.0's projected 420 ppm rise in CO_2. This finding suggests that employing forestation up to the near biophysical limit is unlikely to reduce CO_2 to levels in line with Paris Agreement long-term temperature stabilisation targets when other climate change mitigation measures are not pursued in tandem.

Under strong climate change mitigation SSP1-2.6 conditions (2ºC warming), the additional CDR in Maxforest is lower, with 15 ppm (117 $GtCO_2$) at 2050 and 31 ppm (227 $GtCO_2$) at 2095) (Fig 3E, S12) due to the lower atmospheric CO_2 and moderate reforestation in SSP1-2.6 itself (Fig 1A). However, RF_{net} negates less of this additional CDR (18±12% at 2050; 14±5% at 2095; two model mean with mean uncertainty) than is the case for SSP3-7.0, primarily due to smaller positive RF from surface albedo and methane changes. By 2095, Maxforest's forestation has offset 50% of the projected 52 ppm rise in CO_2 in SSP1-2.6 from 2015, suggesting that when implemented alongside GHG emission reductions, such forestation could contribute to a future where end-of-century CO_2 levels are close to 2015 levels; in contrast to SSP3-7.0.

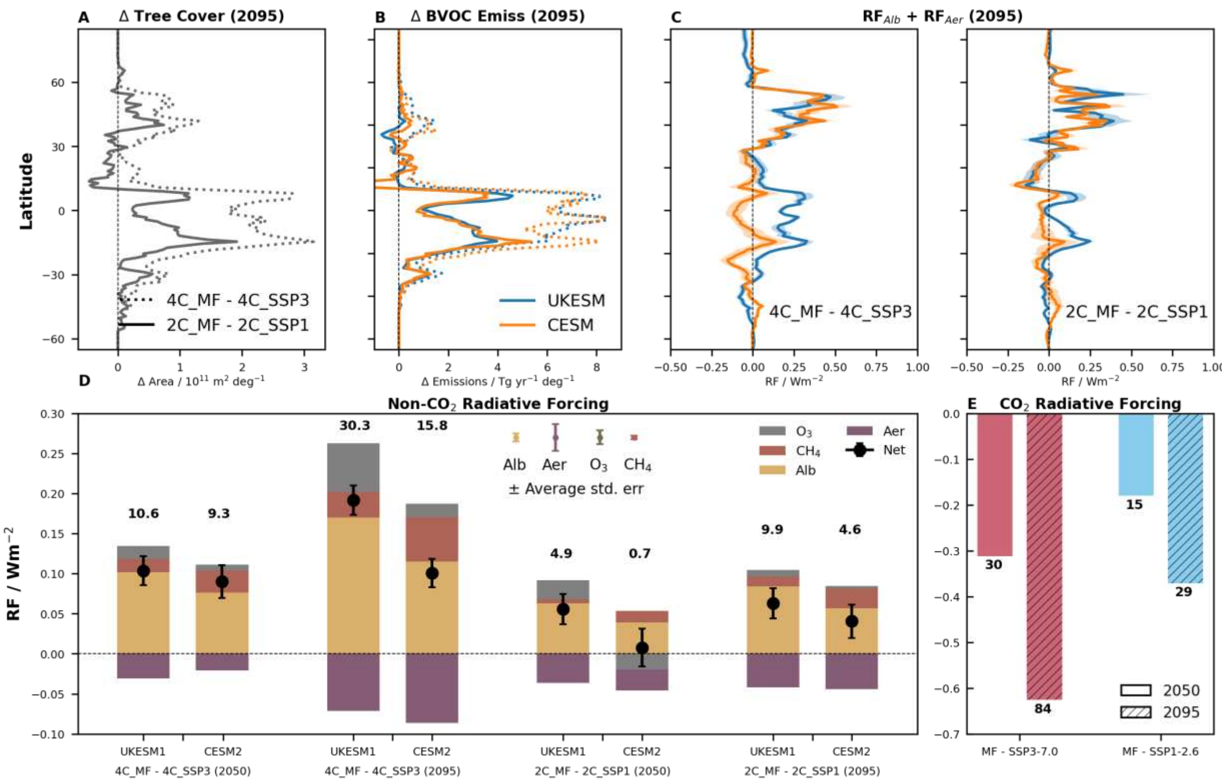

Fig. 3. BVOC emissions, radiative forcing from surface albedo (RF_{Alb}) and aerosol scattering (RF_{Aer}), global mean forcing and CDR differences. Latitudinal changes between 4C_SSP3 and 4C_MF and 2C_SSP1 and 2C_MF (**A**) tree cover and (**B**) BVOC emissions, and (**C**) the sum of RF_{Alb} and RF_{Aer} at 2095 for 4C_MF and 4C_SSP3 and 2C_MF and 2C_SSP1 at 2095 (shading shows standard error in the annual zonal mean). (**D**) Global mean of the non-CO_2 radiative forcing (RF_{net}) and individual RF components (surface albedo, aerosol scattering, CH_4 and O_3), and (**E**) forcing from CO_2 reduction from additional CDR in Maxforest relative to SSP3-7.0 and SSP1-2.6. Bold values show equivalent change in CO_2 (ppm) (**D**) and simulated CO_2 change (ppm) (**E**). Error bars in (**D**) show standard error in the mean.

We note that other mechanisms by which tree cover may affect atmospheric composition, such as fire-related processes (*20*), ozone-induced damage (*19*) and changes in evapotranspiration (*26*), could influence our study's outcomes. While the policy of adding trees where they can thrive was central to the Maxforest scenario's development, certain forested areas may be at a higher risk of wildfires. The exact response is uncertain given the range of drivers including changing temperature and precipitation patterns and population density growth, a change in the vegetation flammability (flammable grassland replaced by less flammable but longer burning trees), and potential forest-driven changes to local moisture. Similarly, changes in surface ozone levels have far-reaching implications for carbon uptake, potentially limiting the capacity for CO_2 removal (19). Moreover, evaporative cooling could be important for surface temperatures in certain regions (*27*). Our modelling setup is a trade-off that balances climate and earth system model parameterization uncertainties while minimising the impact of the complexity of fully coupled interactions.

In conclusion, the changes to atmospheric composition from ozone, methane and aerosol scattering and surface albedo when forest cover is expanded to a near biophysical maximum have a net warming effect which offset up to a third of the CO_2 removal benefit (23-31% under SSP3-7.0 conditions and 14-18% in SSP1-2.6). However, the negative impact is reduced when forestation occurs alongside reduction of emissions of CO_2 and other pollutants. Our results indicate that for forestation to be an effective climate change mitigation strategy, integration with emissions reduction will be required to avoid driving indirect responses in the Earth system that would diminish its cooling potential.

References and Notes

[1] G-J. Nabuurs, R. Mrabet, A. Abu Hatab, M. Bustamante, H. Clark, P. Havlík, J. House, C. Mbow, K.N. Ninan, A. Popp, S. Roe, B. Sohngen, S. Towprayoon.: Agriculture, Forestry and Other Land Uses (AFOLU). In IPCC, 2022: *Climate Change 2022: Mitigation of Climate Change. Contribution of Working Group III to the Sixth Assessment Report of the Intergovernmental Panel on Climate Change* [P.R. Shukla, J. Skea, R. Slade, A. Al Khourdajie, R. van Diemen, D. McCollum, M. Pathak, S. Some, P. Vyas, R. Fradera, M. Belkacemi, A. Hasija, G. Lisboa, S. Luz, J. Malley, (eds.)]. Cambridge University Press, Cambridge, UK and New York, NY, USA. (2022), 10.1017/9781009157926.009

[2] D. Ellison, C. Morris, B. Locatelli, D. Sheil, J. Cohen, D. Murdiyarso, V. Gutierrez, M. Van Noordwijk, I. Creed, J. Pokorny, D. Gaveau,. Trees, forests and water: Cool insights for a hot world. *Global environmental change*, *43*, 51-61 (2017) 10.1016/j.gloenvcha.2017.01.002.

[3] N. Seddon, B. Turner, P. Berry, A. Chausson, C. Girardin.: Grounding nature-based climate solutions in sound biodiversity science. *Nature Climate Change*, *9*(2), 84-87 (2019) 10.1038/s41558-019-0405-0.

[4] J. Syktus, C. McAlpine: More than carbon sequestration: Biophysical climate benefits of restored savanna woodlands. *Scientific Reports 6*, 1 (2016) 10.1038/srep29194.

[5] International Union for the Conservation of Nature (IUCN) Ecosystem restoration https://www.iucn.org/our-work/topic/ecosystem-restoration; last accessed 19th April 2023.

[6] G. Bonan. Forests and Climate Change: Forcings, Feedbacks, and the Climate Benefits of Forests. *Science* 320, 5882, (2008) 10.1126/science.1155121.

[7] S. Rohatyn, D. Yakir, E. Rotenberg, Y. Carmel: Limited climate change mitigation potential through forestation of the vast dryland regions. *Science* 377 1436-1439 (2022), 10.1126/science.abm9684.

[8] G. Thornhill, W. Collins, D. Olivié, R. Skeie, A. Archibald, S. Bauer, R. Checa-Garcia, S. Fiedler, G. Folberth, A. Gjermundsen, L. Horowitz, J-F. Lamarque, M. Michou, J. Mulcahy, P. Nabat, V. Naik, F. O'Connor, F. Paulot, M. Schulz, C. Scott, R. Séférian, C. Smith, T. Takemura, S. Tilmes, K. Tsigaridis, J. Weber: Climate-driven chemistry and aerosol feedbacks in CMIP6 Earth system models. *Atmos. Chem. Phys* 21, 1105–1126, (2012) 10.5194/acp-21-1105-2021.

[9] J. Weber, S. Archer-Nicholls, N.L. Abraham, Y. Shin, P. Griffiths, D. Grosvenor, C. Scott, A. Archibald: Chemistry-driven changes strongly influence climate forcing from vegetation emissions. *Nature Comms* 13,7202 (2022) 10.1038/s41467-022-34944-9.

[10] C. Scott, S. Monks, D. Spracklen, S. Arnold, P. Forster, A. Rap, M. Äijälä, P. Artaxo, K Carslaw, M. Chipperfield, M. Ehn, M.: Impact on short-lived climate forcers increases projected warming due to deforestation. *Nature communications*, *9*(1),157, (2018) 0.1038/s41467-017-02412-4.

[11] N. Unger: Human land-use-driven reduction of forest volatiles cools global climate. *Nature Climate Change* 4, 907–910 (2014), 10.1038/nclimate2347

[12] A. Sellar, C. Jones, J. Mulcahy, Y. Tang, A. Yool, A. Wiltshire, F. O'Connor, M. Stringer, R. Hill, J. Palmieri, S. Woodward, L. de Mora, T. Kuhlbrodt, S. Rumbold, D. Kelley, R. Ellis, C. Johnson, J. Walton, N. Abraham, M. Andrews, T. Andrews, A. Archibald, S. Berthou, E. Burke, E. Blockley, K. Carslaw, M. Dalvi, J. Edwards, G. Folberth, N. Gedney, P. Griffiths, A. Harper, M. Hendry, A. Hewitt, B. Johnson, A. Jones, C. Jones, J. Keeble, S. Liddicoat, O. Morgenstern, R. Parker, V. Predoi, E. Robertson, A. Siahaan, R. Smith, R. Swaminathan, M. Woodhouse, G. Zeng, M. Zerroukat: UKESM1: Description and Evaluation of the U.K. Earth System Model. *Journal of Advances in Modeling Earth System* 11, 4513-4558, (2019) 10.1029/2019MS001739

[13] G. Danabasoglu, J-F. Lamarque, J. Bacmeister, D. Bailey, A. DuVivier, J. Edwards, L. Emmons, J. Fasullo, R. Garcia, A. Gettelman, C. Hannay, C: The community earth system model version 2 (CESM2). *Journal of Advances in Modeling Earth Systems*, 12, 2, (2020), 10.1029/2019MS001916.

[14] S. Roe. “Terrestrial Systems' Impact on and Response to Climate Change” thesis. University of Virginia (2021), doi.org/10.18130/vpyv-gn70.

[15] K. Riahi, D. P. van Vuuren, E. Kriegler, J. Edmonds, B. C. O'Neill, S. Fujimori, N. Bauer, K. Calvin, R. Dellink, O. Fricko, W. Lutz. The Shared Socioeconomic Pathways and their energy, land use, and greenhouse gas emissions implications: An overview. *Glob. Environ. Chang.* 42, 153–168 (2017), 10.1016/j.gloenvcha.2016.05.009.

[16] P. Forster, T. Richardson, A. Maycock, C. Smith, B. Samset, G. Myhre, T. Andrews, R. Pincus, M. Schulz: Recommendations for diagnosing effective radiative forcing from climate models for CMIP6. Journal of Geophysical Research: Atmospheres, 121(20), pp.12-460 (2016), 10.1002/2016JD025320.

[17] A. Guenther, X. Jiang, C. Heald, T. Sakulyanontvittaya, T. Duhl, L. Emmons, X. Wang: The Model of Emissions of Gases and Aerosols from Nature version 2.1 (MEGAN2.1): an extended and updated framework for modeling biogenic emissions. Geosci. Model Dev., 5, 1471–1492, (2012) 10.5194/gmd-5-1471-2012.

[18] J. Weber, J. King, K. Sindelarova, M. Val Martin: Updated Isoprene and Terpene Emission Factors for the Interactive BVOC Emission Scheme (iBVOC) in the United Kingdom Earth System Model (UKESM1.0), Geosci. Model Dev., 16, 3083–3101 (2022) 10.5194/gmd-16-3083-2023.

[19] S. Sitch, P. Cox, W. Collins, C. Huntingford: Indirect radiative forcing of climate change through ozone effects on the land-carbon sink. Nature 448, 791–794 (2007) 10.1038/nature06059.

[20] G. Lasslop, A. Coppola, A. Voulgarakis, C. Yue, S. Veraverbeke: Influence of Fire on the Carbon Cycle and Climate. Curr Clim Change Rep 5, 112–123 (2019) 10.1007/s40641-019-00128-9.

[21] J-F. Bastin, Y. Finegold, C. Garcia, D. Mollicone, M. Rezende, D. Routh, C, Zohner, T. Crowther: The global tree restoration potential. *Science* 365, 6448, (2019), 10.1126/science.aax0848.

[22] R. Betts. Offset of the potential carbon sink from boreal forestation by decreases in surface albedo. *Nature*, *408*, 6809, (2000), 10.1038/35041545.

[23] I. Karset, T., Berntsen, T. Storelvmo, K. Alterskjær, A. Grini, D. Olivié, A. Kirkevåg, Ø; Seland, T. Iversen, M. Schulz. Strong impacts on aerosol indirect effects from historical oxidant changes, *Atmos. Chem. Phys.,* 18, 7669–7690, (2018) 10.5194/acp-18-7669-2018.

[24] A. Lacis, D. Wuebbles, J. Logan: Radiative forcing of climate by changes in the vertical distribution of ozone. *JGR Atmospheres*, 95, 9971-9981 (1990) 10.1029/JD095iD07p09971.

[25] B. Griscom, J. Adams, P. Ellis, R. Houghton, G. Lomax, D. Miteva, W. Schlesinger, D. Shoch, J. Siikamäki, P. Smith, P. Woodbury: Natural climate solutions. *Proc. Natl. Acad. Sci,* 114, 11645-11650 (2017) 10.1073/pnas.1710465114.

[26] L. Boysen, V. Brovkin, J. Pongratz, D. Lawrence, P. Lawrence, N. Vuichard, P. Peylin, S. Liddicoat, T, Hajima, Y. Zhang, M. Rocher, C. Delire, R. Séférian, V. Arora, L. Nieradzik, P. Anthoni, W. Thiery, M. Laguë, D. Lawrence, M.-H. Lo: Global climate response to idealized deforestation in CMIP6 models, Biogeosciences, 17, 5615–5638 (2020) 10.5194/bg-17-5615-2020.

[27] E. Davin, N. de Noblet-Ducoudré: Climatic impact of global-scale deforestation: Radiative versus nonradiative processes. *Journal of Climate*, *23*(1), 97-112, (2009) doi.org/10.1175/2009JCLI3102.1.

[28] J. Weber, LULC input data, Zenodo (2023); https://zenodo.org/records/7657286

[29] J. Weber, UKESM1 data, Zenodo (2023); https://zenodo.org/records/7691836

[30] J. Weber, CESM2 data, Zenodo (2023); https://zenodo.org/records/7692341

[31] J. Weber, CLM5 land carbon data, Zenodo (2023); https://zenodo.org/records/7689779

[32] J. Weber Additional CESM and UKESM data and plotting code, Zenodo (2023); https://zenodo.org/records/8338308

[33] J.Weber, Code for making the figures, Zenodo (2023); https://zenodo.org/records/7851079

[34] W. Collins, J.-F. Lamarque, M. Schulz, O. Boucher, V. Eyring, M. Hegglin, A. Maycock, G. Myhre, M. Prather, D. Shindell, S. Smith.: AerChemMIP: quantifying the effects of chemistry and aerosols in CMIP6, Geosci. Model Dev., 10, 585–607, (2017) 10.5194/gmd-10-585-2017.

[35] F. O'Connor, N Abraham, M Dalvi, G. Folberth, P. Griffiths, C. Hardacre, B. Johnson, R. Kahana, J. Keeble, B. Kim, O. Morgenstern, J. Mulcahy, M. Richardson, E. Robertson, J. Seo, S. Shim, J. Teixeira, S. Turnock, J. Williams, A. Wiltshire, S. Woodward, and G. Zeng: Assessment of pre-industrial to present-day anthropogenic climate forcing in UKESM1, *Atmos. Chem. Phys.,* 21, 1211–1243, (2021), 10.5194/acp-21-1211-2021.

[36] B. O'Neill, C. Tebaldi, D. van Vuuren, V. Eyring, P. Friedlingstein, G. Hurtt, R. Knutti, E., Kriegler, J-F. Lamarque, J. Lowe, G. Meehl, R. Moss, K. Riahi, B. Sanderson: The Scenario Model Intercomparison Project (ScenarioMIP) for CMIP6, *Geosci. Model Dev* 9, 3461–3482 (2016) 10.5194/gmd-9-3461-2016.

[37] D. Lawrence, R. Fisher, C. Koven, K. Oleson, S. Swenson, G. Bonan, N. Collier et al. The Community Land Model version 5: Description of new features, benchmarking, and impact of forcing uncertainty. *Journal of Advances in Modeling Earth Systems* 11, 12, 4245-4287 (2019) 10.1029/2018MS001583.

[38] L. Emmons, J. Orlando, G. Tyndall, R. Schwantes, D. Kinnison, D. Marsh, M. Mills, S. Tilmes., J-F. Lamarque: The MOZART Chemistry Mechanism in the Community Earth System Model version 2 (CESM2). *J. Adv. Model. Earth Syst*, *12*, 10.1029, (2020), 10.1029/2019MS001882.

[39] X. Liu, P-L. Ma, H. Wang, S. Tilmes, B. Singh, R. Easter, S. Ghan, P. Rasch: Description and evaluation of a new four-mode version of the Modal Aerosol Module (MAM4) within version 5.3 of the Community Atmosphere Model, *Geosci. Model Dev.*, 9, 505–522 (2016) 10.5194/gmd-9-505-2016.

[40] S. Tilmes, J.-F. Lamarque, L. Emmons, D. Kinnison, P-L. Ma, X. Liu, S. Ghan, C. Bardeen, S. Arnold, M. Deeter, F. Vitt, T. Ryerson, J. Elkins, F. Moore, J. Spackman, M. Val Martin.: Description and evaluation of tropospheric chemistry and aerosols in the Community Earth System Model (CESM1.2), *Geosci. Model Dev.,* 8, 1395–1426, (2015), 10.5194/gmd-8-1395-2015.

[41] J. Weber, S. Archer-Nicholls, N. Abraham, Y. Shin, T. Bannan, C. Percival, A. Bacak, P. Artaxo, M. Jenkin, M. Khan, D. Shallcross, R. Schwantes, J. Williams, A. Archibald: Improvements to the representation of BVOC chemistry–climate interactions in UKCA (v11.5) with the CRI-Strat 2 mechanism: incorporation and evaluation, *Geosci. Model Dev.,*14, 5239–5268, (2021) 10.5194/gmd-14-5239-2021.

[42] G. Mann, K. Carslaw, D. Spracklen, D. Ridley, P. Manktelow, M. Chipperfield, S. Pickering, C. Johnson. Description and evaluation of GLOMAP-mode: a modal global aerosol microphysics model for the UKCA composition-climate model, Geosci. Model Dev., 3, 519–551 (2010) 10.5194/gmd-3-519-2010.

[43] J. Olivier, J. Peters, C. Granier, G. Petron, J-F. Muller, S. Wallens: Present and future surface emissions of atmospheric compounds, POET Report #3, EU project EVK2-1999-00011,

(2003) available at: http://www.aero.jussieu.fr/projet/ACCENT/Documents/del2_final.doc (last accessed: 29 December 2022).

[44] J. Weber, S. Archer-Nicholls, P. Griffiths, T. Berndt, M. Jenkin, H. Gordon, C. Knote, A. Archibald. CRI-HOM: A novel chemical mechanism for simulating highly oxygenated organic molecules (HOMs) in global chemistry–aerosol–climate models, Atmos. Chem. Phys., 20, 10889–10910 (2020), 10.5194/acp-20-10889-2020.

[45] P. Durack, K. Taylor, Karl V. Eyring, S. Ames, C. Doutriaux, T. Hoang, D. Nadeau, M. Stockhause, P. Gleckler, input4MIPs: Making [CMIP] model forcing more transparent. United States: (2017) 10.2172/1463030.

[46] F. Pacifico, S. Harrison, C. Jones, A. Arneth, S. Sitch, G Weedon, M. Barkley, P. Palmer, D. Serça, M. Potosnak, T-M. Fu, A. Goldstein, J. Bai, G. Schurgers.: Evaluation of a photosynthesis-based biogenic isoprene emission scheme in JULES and simulation of isoprene emissions under present-day climate conditions, *Atmos. Chem. Phys.,* 11, 4371–4389, (2011), 10.5194/acp-11-4371-2011.

[47] J-F. Lamarque, L. Emmons, P. Hess, D. Kinnison, S. Tilmes, F. Vitt, C. Heald, E. Holland, P. Lauritzen, J. Neu, J. Orlando, P. Rasch, G. Tyndall.: CAM-chem: description and evaluation of interactive atmospheric chemistry in the Community Earth System Model, *Geosci. Model Dev*., 5, 369–411, (2012) 10.5194/gmd-5-369-2012, 2012.

[48] G. Meehl, C. Senior, V. Eyring, G. Flato, J.-F. Lamarque, R. Stouffer, K. Taylor, M. Schlund: Context for interpreting equilibrium climate sensitivity and transient climate response from the CMIP6 Earth system models. *Science Advances* 6, 26 (2020) 10.1126/sciadv.aba1981.

[49] D. Grosvenor, P. Field, A. Hill, B Shipway. The relative importance of macrophysical and cloud albedo changes for aerosol-induced radiative effects in closed-cell stratocumulus: insight from the modelling of a case study. *Atmospheric Chemistry and Physics* 17.8, 5155-5183 (2017), 10.5194/acp-17-5155-2017.

[50] D. Grosvenor, K. Carslaw. The decomposition of cloud–aerosol forcing in the UK Earth System Model (UKESM1), A*tmospheric Chemistry and Physics* 20, 15681–15724 (2020), 10.5194/acp-20-15681-2020.

[51] J. Seinfeld, S. Pandis. Atmospheric Chemistry and Physics: From Air Pollution to Climate Change. 2nd Edition, (John Wiley & Sons, New York, 2006).

[52] C. Seethala, A. Horváth. Global assessment of AMSR-E and MODIS cloud liquid water path retrievals in warm oceanic clouds. *Journal of Geophysical Research: Atmospheres* 115.D13 (2010), 10.1029/2009JD012662.

[53] N. Leach, S. Jenkins, Z. Nicholls, C. Smith, J. Lynch, M. Cain, T. Walsh, B. Wu, J. Tsutsui,M. Allen. FaIRv2.0.0: a generalized impulse response model for climate uncertainty and future scenario exploration, *Geosci. Model Dev.*, 14, 3007–3036 (2021), 10.5194/gmd-14-3007-2021.

[54] D. Lawrence, G. Hurtt, A. Arneth, V. Brovkin, K. Calvin, A. Jones, C. Jones, P. Lawrence, N. de Noblet-Ducoudré, J. Pongratz, S. Seneviratne, E. Shevliakova. The Land Use Model Intercomparison Project (LUMIP) contribution to CMIP6: rationale and experimental design, Geosci. Model Dev., 9, 2973–2998, (2016) 10.5194/gmd-9-2973-2016.

[55] M. Etminan, G. Myhre, E. Highwood, K. Shine: Radiative forcing of carbon dioxide, methane, and nitrous oxide: A significant revision of the methane radiative forcing. *Geophysical Research Letters*, 43, 24 (2016), 10.1002/2016GL071930.

[56] S. Ghan: Technical Note: Estimating aerosol effects on cloud radiative forcing. *Atmos. Chem. Phys.*, 13, 9971–9974, (2013) 10.5194/acp-13-9971-2013.

[57] C. Holmes: Methane feedback on atmospheric chemistry: Methods, models, and mechanisms. *Journal of Advances in Modeling Earth Systems*, 10, 4 (2018), 10.1002/2017MS001196.

[58] C. Smith, R. Kramer, G. Myhre, P. Forster, B. Soden, T. Andrews, O. Boucher, G. Faluvegi, D. Fläschner, Ø. Hodnebrog, M. Kasoar.:. Understanding rapid adjustments to diverse forcing agents. *Geophysical Research Letters*, *45*, 21, 12-023, 10.1029/2018GL079826, 2018.

[59] R. Skeie, G. Myhre, Ø. Hodnebrog, P. Cameron-Smith, M. Deushi, M. Hegglin, L. Horowitz, R. Kramer, M. Michou, M. Mills, D. Olivié: Historical total ozone radiative forcing derived from CMIP6 simulations. *Npj Climate and Atmospheric Science*, 3, 1 (2020), 10.1038/s41612-020-00131-0.

Acknowledgments:.

Funding:

UKRI Future Leaders Fellowship Programme awarded to MVM (MR/T019867/1) supporting JW and JAK.

High-performance computing support from Cheyenne (doi:10.5065/D6RX99HX) was provided by NCAR's Computational and Information Systems 650 Laboratory, sponsored by the National Science Foundation.

This work used Monsoon2, a collaborative high-performance computing facility funded by the Met Office and the Natural Environment Research Council. This work used JASMIN, the UK collaborative data analysis facility.

University of Cambridge ESS-DT (YMS).

NERC/IIASA Collaborative Research Fellowship awarded to CJS (NE/T009381/1).

We gratefully acknowledge funding from the Leverhulme Trust, (Leverhulme Research Centre grant RC-2015-029, DJB).

We thank Prof. Colin Osborne and Prof. Dave Edwards for their comments and advice on the manuscript.

Author contributions:

Conceptualization: JW, JK, MVM, DJB, SR

Methodology: JW, JK, MVM, NLA, YMS, CJS, PL, SR

Investigation: JW, JK, DPG

Visualization: JW, JK, MVM, DJB

Funding acquisition: MVM

Project administration: MVM

Supervision: MVM

Writing – original draft: JW

Writing – review & editing: JW, MVM, DJB, JK, SR

Competing interests:

DJB has a minority equity stake in Future Forest/Undo.

JAK sits on the advisory panel for Ecologi, an organisation which invests in ecosystem restoration projects.

All other authors declare that they have no competing interests.

Data and materials availability:

Model data from UKESM1, CESM2 and CLM5 are available from the following repositories. All the data are freely available.

(28) LULC input data: https://doi.org/10.5281/zenodo.7657286

(29) UKESM1 data: https://doi.org/10.5281/zenodo.7691836

(30) CESM2 data: https://doi.org/10.5281/zenodo.7692341

(31) CLM5 land carbon data: https://doi.org/10.5281/zenodo.7689779

(32) Additional CESM and UKESM data and plotting code: https://doi.org/10.5281/zenodo.8338308

Input emissions from SSP3-7.0 and SSP1-2.6 are available from the input4MIPs repository (https://esgf-node.llnl.gov/projects/input4mips/) maintained by ESGF.

(33) Code for making the figures: https://doi.org/10.5281/zenodo.7851079

The CESM2 code is freely available online and can be downloaded at https://www.cesm.ucar.edu/cesm2 (last accessed 1st August 2023). Due to intellectual property right restrictions, we cannot provide either the source code or documentation papers for the Unified Model/UKESM. The Met Office Unified Model/UKESM is available for use under licence. For further information on how to apply for a licence, see https://www.metoffice.gov.uk/research/approach/modelling-systems/unified-model (last accessed 1st August 2023). Suite numbers for the runs are listed in the README which accompanies the UKESM1 data repository on Zenodo.

Supplementary Materials

Materials and Methods

Figs. S1 to S12

Tables S1 to S2

References (34-59)

Table 1. Modelling Experiments in UKESM1 and CESM2.

Simulations[a]	**Land Surface Cover (forest cover change at 2095 relative to 2015)**	**Simulation Conditions[b]**	**ΔGlobal Tree Cover (MF - SSP) at 2050 (2095)**	**ΔBVOC Emissions (MF - SSP) at 2050 (2095)[c]**
4C_SSP3	SSP3 (deforestation, -290 Mha)	SSP3-7.0 (High warming up to 4ºC, small air pollution decrease)	15% (26%)	17-19% (32-38%)
4C_MF	Maxforest (extensive forestation, +750 Mha)			
2C_SSP1	SSP1 (forestation, +300 Mha)	SSP1-2.6 (Low warming up to 2ºC, large air pollution decrease)	6% (10%)	8% (11-13%)
2C_MF	Maxforest (extensive forestation, +750 Mha)			

[a]Simulations performed at 2050 and 2095
[b]Well-mixed GHGs, anthropogenic and biomass burning emissions, and sea-surface temperatures.
[c]Range shows model variation.